Identification of Magnetic Bearing Stiffness and Damping Based on Hybrid Genetic Algorithm

Zhao Chen[1], *Zhou Jin*[1*], *Xu Yuanping*[1], *Di Long*[2], *Ji Minlai*[3]

1 College of Mechanical and Electrical Engineering, Nanjing University of Aeronautics and Astronautics, Nanjing 210016, P. R. China;
2 Rotating Machinery and Control Laboratory (ROMAC), University of Virginia, Charlottesville, VA 22904, USA;3 AVIC Radar and Electronic Equipment Research Institute, Suzhou 215000, P. R. China

(Received 15 May 2015; revised 15 December 2016; accepted 22 January 2017)

Abstract: Identifying the stiffness and damping of active magnetic bearings (AMBs) is necessary since those parameters can affect the stability and performance of the high-speed rotor AMBs system. A new identification method is proposed to identify the stiffness and damping coefficients of a rotor AMB system. This method combines the global optimization capability of the genetic algorithm (GA) and the local search ability of Nelder-Mead simplex method. The supporting parameters are obtained using the hybrid GA based on the experimental unbalance response calculated through the transfer matrix method. To verify the identified results, the experimental stiffness and damping coefficients are employed to simulate the unbalance responses for the rotor AMBs system using the finite element method. The close agreement between the simulation and experimental data indicates that the proposed identified algorithm can effectively identify the AMBs supporting parameters.

Key words: magnetic bearing; hybrid genetic algorithm; bearing parameters; finite element model

CLC number: TP273 **Document code**: A **Article ID**: 1005-1120(2017)02-0211-09

0 Introduction

Compared with the traditional mechanical bearings, active magnetic bearings (AMBs) are nearly no friction and free of lubrication. Therefore, AMBs have been increasingly used in turbo machinery and aerospace applications. The stiffness and damping of AMBs affect the stability and performance of high-speed rotor AMBs system and the identification for these values is important. Several methods have been developed for the mechanical bearing identification and most of these approaches use the least squares method based on kinetic equations[1]. Santiago et al.[2] identified the stiffness and damping coefficients of two sliding bearings using impact and imbalance excitation. By comparing results of the two methods, the imbalance excitation method is more robust. Meanwhile, Andrés et al.[3] identified the bearing force coefficients from measurements of imbalance response of a flexible rotor. But accuracy of the results is closely related to the size of global (rotor) mass, stiffness and gyroscopic matrices. Tiwari et al.[4] presented an identification algorithm for simultaneous estimation of residual unbalances and bearing dynamic parameters. The standard condensation method is used to reduce the number of degrees of freedom (DOFs) of the model and the identified parameters are closely agreed with the assumed parameters used in the simulation. Knaapen[5] used instrumental variables to optimize the final values of AMBs' stiffness and damping coefficients and the results based on instrumental variables are better than those of the least square method.

The stiffness and damping coefficients of AMBs have a significant influence on the dynamic

* Corresponding author, E-mail address: zhj@nuaa.edu.cn.

How to cite this article: Zhao Chen, Zhou Jin, Xu Yuanping, et al. Identification of magnetic bearing stiffness and damping based on hybrid genetic algorithm[J]. Trans. Nanjing Univ. Aero. Astro., 2017,34(2):211-219.
http://dx.doi.org/10.16356/j.1005-1120.2017.02.211

response of a rotor bearing system, ranging from the bending critical speeds, modes of vibrations and stability. Due to the special structures of AMBs, the traditional method based on dynamic equations cannot be applied directly. Therefore, many researchers[6-9] proposed different methods to identify the supporting parameters. In a rotor AMB system, the deformation of the flexible rotor becomes more obviously with the increasing speed, which makes it more difficult to identify the supporting parameters. The algorithms need the gradient information of the objective function with respect to the design variables and the solutions cannot get out of local optimum points when they fall in. Besides, this algorithm may skip the global optimum solution because they depend on the primitive values and may converge to a local optimum solution which is near the starting point. Experience and time are required to overcome these disadvantages. Many search algorithms have been developed to overcome the drawbacks. For global optimization, one of the most popular algorithms is genetic algorithm (GA), which was described by Ying et al.[10] and other researchers[11-13].

GA is a stochastic search technique based on the mechanism of natural selection and genetics, and it does not need the mathematical requirements for the solution. This algorithm possesses more flexibility characteristics than other methods using a single-point search, but lower efficiency. Nelder-Mead Simplex method[14] is a direct optimization algorithm with powerful local search ability, but it may fall into a local optimum. In this paper, one optimization method that combines the global optimization capability of GAs and Nelder-Mead simplex local search ability is proposed to identify the stiffness and damping coefficients of AMBs, which will speed up computation greatly and find the global optimal solutions more effectively. Once GA locates the candidate solutions, we make the candidate solutions as initial values for the local search algorithm, which will effectively search the local optimal solutions that correspond to the termination condition. From the comparisons between finite element response and experimental measurements, the proposed hybrid GA can effectively identify the stiffness and damping coefficients of AMBs.

In this method, the first step is to calculate the residual function $R(p)$, which is the differences values between the theoretical imbalance response by the transfer matrix method[15] and the experimental data. Optimization of the residual function is the second step in identification of AMB stiffness and damping. Since the appropriate optimization algorithm not only can ensure the accuracy of the bearing parameters, but also improve the calculation efficiency, we propose the hybrid GA, which combines the global optimization capability with high efficiency.

1 Basic Parameter Identification Principle of AMBs

1.1 Rotor AMB system

The test rig for identification is shown in Fig. 1(a). Fig. 1(b) shows the rotor structure of AMBs system[16-17]. The proportional-integral-de-

(a) Rotor-AMB system

(b) Rotor employed in this system

Fig. 1 Rotor-AMB system and rotor employed in this system

rivative(PID) control strategy controller is employed to control the magnetic bearing system. For the PID controller, its transfer function $G(s)$ can be written as

$$G(s) = C_p + C_d s + \frac{C_i}{s}$$

where C_p is the proportional coefficient, C_d the derivative coefficient, and C_i the integral coefficient.

The steel shaft is 436 mm long with a main diameter of 39.8 mm. Table 1 describes physical properties of the rotor. The AMBs employed in this paper is shown in Fig. 2. Two pairs of eddy current displacement sensors, that are orthogonally positioned, record the rotor displacements near each AMB location. Fig. 3 shows the positioning of the displacement sensors and their axial location, where x_1, y_1, x_2, y_2 are the displacement for both AMBs at two orthogonal direction. Signals from the displacement sensors are directed to an industrial-type data acquisition system connected to a PC.

Table 1 Physical properties of rotor

Parameter	Values
Rotor length/mm	436
Rotor mass/kg	2.4
Density/(kg·m^{-3})	7 850
Young's modulus/GPa	209
Shaft diameter at bearing location/mm	39.8
Distance from left sensor to bearing/mm	26
Distance of two AMB/mm	312

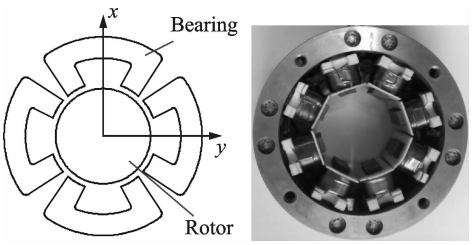

Fig. 2 Radial bearing

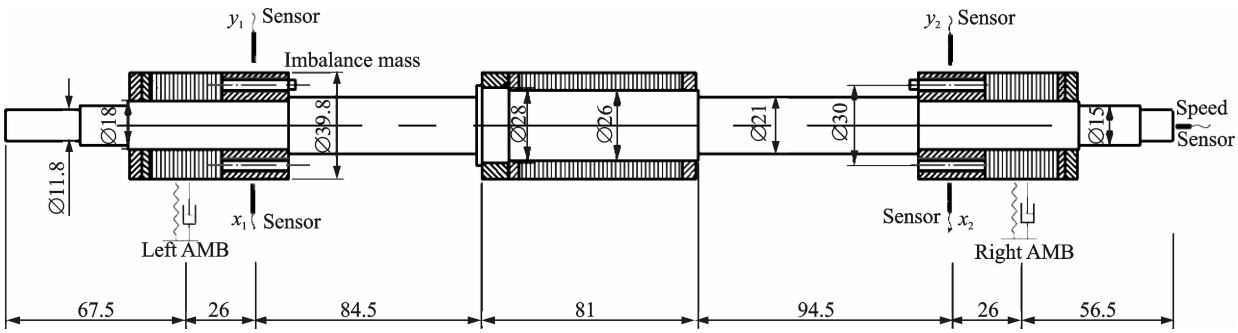

Fig. 3 Locations of displacement sensors, magnetic bearings and imbalance planes, and test rotor geometry

The experiment of adding imbalance excitation is conducted to verify the results. The rotor operates within a certain speed range from 1 200 r/min to 15 600 r/min. The experiment procedures start with designing a feedback controller to stabilize the rotor with AMBs, such as a PID controller, inject sinusoidal excitation signal using a signal generator, increase the excitation frequency to 300 Hz, inspect the displacement signal in LABVIEW, and verify whether the controller can handle unbalance force with 300 Hz frequency. After safety inspection, turn on the inverter and adjust the motor speed. The displacement signals are obtained by NI DAQ and saved every 600 r/min from 1 200 r/min to 15 600 r/min using LABVIEW interface. After Kaiser band pass filtering and Fourier transform, the imbalance response amplitude and phase are extracted from the initial displacement data, which are used to identify the AMB parameters in terms of corresponding frequency.

1.2 Basic principles of hybrid GA based on unbalance response

The classical GA is a method of global optimization, but the global algorithm lacks the local search capability. Search operations are repeated in the vicinity of the genetic optimal solution, which results in low accuracy. Nelder-Mead simplex method is a direct optimization algorithm with powerful local search ability. But reasonable

initial values should be provided to obtain the optimal solution. Besides, the supporting parameters corresponding to different frequencies are quite different in AMB system, which makes the initial value selection more difficult. For the optimization algorithm applied to the AMB supportting parameter identification, it is very important to select a objective function that plays a critical role in the final identification results. The following process describes how to calculate the fitness function.

Ref. [18] has already detailed the rotor modeling, model updating and rectified model verification. Here, the rectified rotor model is employed directly to calculate the AMB dynamic parameters. The Riccati Transfer Matrix Method is adopted to calculate the displacement state vector. The state equations of the overall system are defined as

$$\boldsymbol{Z}_N = \boldsymbol{T}_1 \boldsymbol{T}_2 \cdots \boldsymbol{T}_{N-1} \boldsymbol{Z}_1 \tag{1}$$

where $\boldsymbol{T}_1, \boldsymbol{T}_2, \cdots, \boldsymbol{T}_N$ represent the transfer matrix for the entire system. $\boldsymbol{Z}_1$ represents the generalized state vector of initial state vector of the first section (including generalized displacement and force), $\boldsymbol{Z}_N$ the generalized state vector of the last section. The relation of the state vector $\boldsymbol{Z}_{i+1}$ and $\boldsymbol{Z}_i$ is defined as

$$\boldsymbol{Z}_{i+1} = \begin{Bmatrix} \boldsymbol{f} \\ \boldsymbol{e} \end{Bmatrix}_{i+1} = \begin{bmatrix} \boldsymbol{T}_{11} & \boldsymbol{T}_{12} \\ \boldsymbol{T}_{21} & \boldsymbol{T}_{22} \end{bmatrix}_i \begin{Bmatrix} \boldsymbol{f} \\ \boldsymbol{e} \end{Bmatrix}_i + \begin{Bmatrix} \boldsymbol{F}_{\mathrm{f}} \\ \boldsymbol{F}_{\mathrm{e}} \end{Bmatrix}_i \tag{2}$$

where the generalized load vector $\boldsymbol{f}$ is obtained from the imbalance distribution and the vector $\boldsymbol{e}$ the displacement state vector. $\boldsymbol{F}_{\mathrm{f}}$ is the external force and $\boldsymbol{F}_{\mathrm{e}}$ the displacement vector. The matrix $\boldsymbol{T}_{12}$ is defined as

$$\boldsymbol{T}_{12} = \begin{bmatrix} 0 & -I_{\mathrm{d}}\omega^2 & 0 & \mathrm{i}I_{\mathrm{p}}\omega^2 \\ m\omega^2 - K_{xx} - \mathrm{i}C_{xx}\omega & 0 & 0 & 0 \\ 0 & -\mathrm{i}I_{\mathrm{p}} & 0 & -I_{\mathrm{d}}\omega^2 \\ 0 & 0 & m\omega^2 - K_{yy} - \mathrm{i}C_{yy}\omega & 0 \end{bmatrix} \tag{3}$$

where $\boldsymbol{T}_{11}, \boldsymbol{T}_{22}$ are the 4×4 identity matrix, $\boldsymbol{T}_{21}$ is the zero matrix. I_{p} is the polar moment of inertia and I_{d} the transverse moment of inertia. K_{xx} and C_{xx} are the stiffness and damping coefficients in x direction, K_{yy} and C_{yy} the stiffness and damping coefficients in y direction. ω represents the rotating speed and m the mass of rotor. In the same section, the relationship between the force vector $\boldsymbol{f}_i$ and displacement vector $\boldsymbol{e}_i$ is defined as

$$\boldsymbol{f}_i = \boldsymbol{S}_i \boldsymbol{e}_i + \boldsymbol{P}_i \tag{4}$$

where $\boldsymbol{S}_i$ is the transfer matrix of the ith section and $\boldsymbol{P}_i$ the force vector. According to the Eqs. (2) and (4), the recursive formula of $\boldsymbol{S}_i$, $\boldsymbol{P}_i$ and the inverse recursive formula of $\boldsymbol{e}_i$ can be obtained as

$$\begin{aligned} \boldsymbol{S}_{i+1} &= [\boldsymbol{T}_{11}\boldsymbol{S} + \boldsymbol{T}_{22}]_i [\boldsymbol{T}_{21}\boldsymbol{S} + \boldsymbol{T}_{22}]_i^{-1} \\ \boldsymbol{P}_{i+1} &= [\boldsymbol{T}_{11}P + \boldsymbol{F}_{\mathrm{f}}]_i - \boldsymbol{S}_{i+1}[\boldsymbol{T}_{21}\boldsymbol{P} + \boldsymbol{F}_{\mathrm{e}}]_i \end{aligned} \tag{5}$$

$$\boldsymbol{e}_i = [\boldsymbol{T}_{21}\boldsymbol{S} + \boldsymbol{T}_{22}]_i^{-1} \boldsymbol{e}_{i+1} - [\boldsymbol{T}_{21}\boldsymbol{S} + \boldsymbol{T}_{22}]_i^{-1} [\boldsymbol{T}_{21}\boldsymbol{P} + \boldsymbol{F}_e]_i \tag{6}$$

In the process of solving the displacement vectors, at certain excitation frequency ω_j, the displacement state vector $\boldsymbol{e}_{mj}$ can be obtained at frequencies ω_j based on the state vector of the two ends and Eq. (6).

The residual vectors calculated from experiment and transfer matrix at frequency ω_j are defined as

$$\begin{aligned} \boldsymbol{\varepsilon}_A(\boldsymbol{p}) &= |\boldsymbol{A}(e_{Bj}) - \boldsymbol{A}(e_{Aj})|^2 \\ \boldsymbol{\varepsilon}_P(\boldsymbol{p}) &= |\boldsymbol{P}(e_{Bj}) - \boldsymbol{P}(e_{Aj})|^2 \end{aligned} \tag{7}$$

where $\boldsymbol{p}$ is the correction vector. $\boldsymbol{A}(e_{Bj})$ and $\boldsymbol{A}(e_{Aj})$ are the unbalance response amplitude, and $\boldsymbol{P}(e_{Bj})$ and $\boldsymbol{P}(e_{Aj})$ the unbalance response phase vectors of the rotor movement obtained in experiment and calculated through transfer matrix at speed ω_j. The residual amplitude vector at frequency ω_j is defined as $\boldsymbol{\varepsilon}_A(\boldsymbol{p})$ and $\boldsymbol{\varepsilon}_P(\boldsymbol{p})$ the residual phase vector. The fitness function is defined as

$$\begin{aligned} &\mathrm{Min}R(\boldsymbol{p}), R(\boldsymbol{p}) = K_A(j)\boldsymbol{\varepsilon}_A(\boldsymbol{p}) + K_P(j)\boldsymbol{\varepsilon}_P(\boldsymbol{p}) \\ &\text{s. t.} \qquad L_B \leqslant \boldsymbol{p} \leqslant U_B \end{aligned} \tag{8}$$

where L_B and U_B represent the upper and lower bound of correction parameters, and $K_A(j)$ and $K_P(j)$ the weighting factors. The fitness function of this model is the same as Eq. (8).

1.3 Residual optimization based on hybrid GA

The proposed hybrid GA has two main processes, the global search and the local search,

as shown in Fig. 4. Groups of candidates for optimum solutions are determined by the global search component.

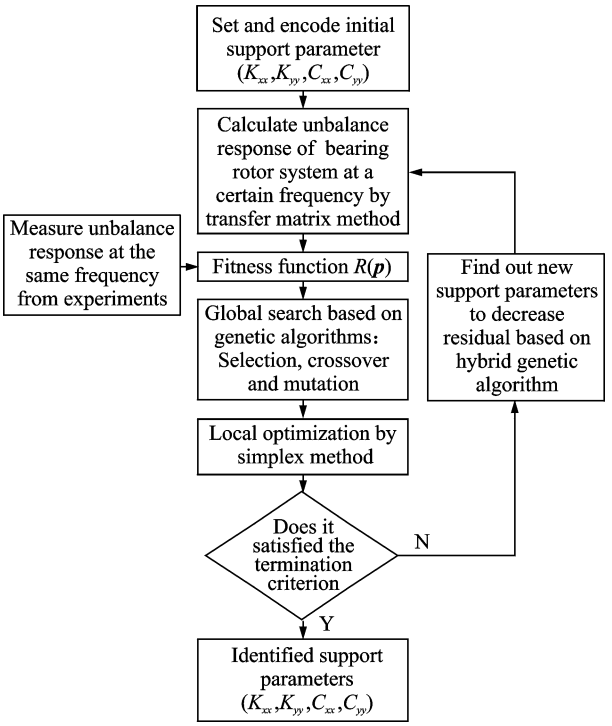

Fig. 4 AMB parameter identification process based on hybrid GA

The modified simplex method is used in the local search component. Hybrid GA combines the advantages of both classical GA and simplex global local search, which greatly improves the accuracy of search process. The specific steps are summarized as follows:

Step 1 Produce individuals using the genetic uniform distribution method.

Step 2 Generate the initial solutions in parameter range and calculate the fitness function.

Step 3 Select candidate solutions by operating procedures of GA(selection, crossover, mutation).

Step 4 Search the optimum solutions by the simplex method.

Step 5 Determine the final optimum solution by the termination condition.

1.3.1 Global search (Steps 1—3)

Initial population should be randomly generated by selecting 100 individuals from all AMB parameters with binary encoding according to previous experience

$$H_{\min} \leqslant H_j \leqslant H_{\max} \quad j=1,2,\cdots \tag{9}$$

where $H_{\min}$ and $H_{\max}$ are the upper and lower bounds of AMB parameters. Initial population should be randomly generated by initial population coding within the range. The initial population size $M = 100$ and the maximum evolution generation $T = 200$. The selected fitness function, which is the residual vector between test and transfer matrix results, has a significant influence on the final calculation results. The weighting factors $K_A(j)$ and $K_P(j)$ are used to describe each parameter as

$$f(x_j)=R(\boldsymbol{p})=K_A(j)\boldsymbol{\varepsilon}_A(\boldsymbol{p})+K_P(j)\boldsymbol{\varepsilon}(\boldsymbol{p}) \tag{10}$$

A linear scaling approach is proposed to reduce the amount of unnecessary calculations and to prevent premature convergence. Select the high fitness individuals by roulette wheel from AMB parameter groups. The better code sequence are chosed from random pair of groups. Then we exchange from a certain position of the two-bit code string to improve the operation speed by single-point method or two-point method. Non-uniform mutation changes one of the parameters of based on a non-uniform probability distribution. The search strategy and parameters for GA are shown in Table 2.

Table 2 Search strategy and parameters for GA

GA strategy	Type or values
Population size	100
Selection type	Roulette wheel
Crossover type and probability	One- and two-point crossover, 50%
Mutation type	Dynamic mutation
Maximum generation	200 or ending condition

1.3.2 Local search (Steps 4,5)

Set initial values as the supporting parameters identified by GA for Nelder-Mead simplex method and perform intensive search to determine the highest and lowest points for a given vertex function in simplex algorithm, and then form a new simplex through a series of reflection, expansion and compression operations, thereby gradually converge to the optimal solution, after-

wards construct a N-dimensional simplex with $N+1$ vertices. The function values of simplex vertices are sorted to satisfy

$$f(x_1^{(k)}) \leqslant f(x_2^{(k)}) \leqslant \cdots \leqslant f(x_{n+1}^{(k)}) \quad (11)$$

where n is the dimension of the parameter, k the number of iterations. $f(x_i^{(k)})$ $(i=1,2,\cdots,n)$ represents the point value of the fitness function $(R(\boldsymbol{p}))$ which determines the best point, the worst point and the suboptimal point. The reflection, compression and expansion coefficients are respectively defined as α,β,γ to satisfy

$$\begin{aligned} x_r^{(k)} &= x_c^{(k)} + \alpha(x_c^{(k)} - x_{n+1}^{(k)}) \\ x_s^{(k)} &= x_c^{(k)} + \beta(x_h^{(k)} - x_c^{(k)}) \\ x_e^{(k)} &= x_c^{(k)} + \gamma(x_{n+1}^{(k)} - x_c^{(k)}) \end{aligned} \quad (12)$$

where $f(x_h^{(k)}) = \min\{f(x_{n+1}^{(k)}), f(x_r^{(k)})\}$, $x_c^{(k)}$ represents the center of simplex, $f(x_c^{(k)})$ the function value at the center of simplex. Compared with the conventional GA, hybrid GA is more stable and accurate. To make up for poor post-search capability and shortcomings of prematurity of GA, termination criterion based on hybrid GA is chosen as

$$\left\{\frac{1}{n+1}\sum_{i=1}^{n+1}[f(x_i^{(k)}) - f(x^{(k)})]^2\right\}^{1/2} \leqslant \varepsilon \quad (13)$$

where ε represents the accuracy set in advance. If the fitness function is not satisfied with setting accuracy, it returns to Step 1 and continues to generate a new iteration of the supporting parameter calculation. If the fitness function meets the accuracy requirements, the optimal solution will be the supporting identification parameters.

2 Imbalance Response Measurement and Identification of Bearing Parameters

The experimental unbalance responses are collected from the flexible rotor-AMBs test rig described in Section 1.1. The unbalance mass used in the experiment is fixed with different types M3 screw. The specifications are shown in Table 3. The data logging starts from 1 200 r/min to 15 600 r/min. The rotor displacements and rotating speed information are saved every 300 r/min for 10 s. Afterwards, the measured displacements go through unbalance signal filtering using Kaiser band-pass filters and zero phase digital filters to extract the steady state amplitude and phase information, which are shown in Figs. 5, 6. x_1, y_1, x_2 and y_2 are the unbalance responses values at each AMBs for two orthogonal direction.

Table 3 Unbalanced mass and installation location in experiment

Disk	Mass/g	Phase/(°)	Radius/mm
Left	0.785 0	0	15
Right	0.981 2	0	15

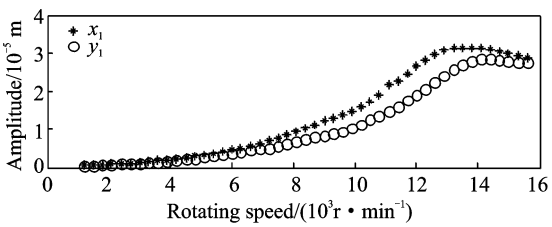

(a) Experimental amplitude information for x and y axes of Left AMB

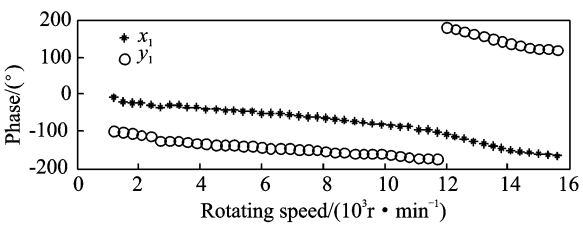

(b) Experimental phase information for x and y axes of Left AMB

Fig. 5 Experimental amplitude and phase information for x and y axes of Left AMB

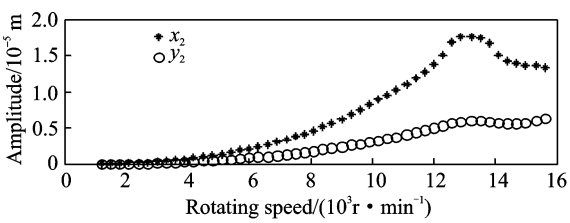

(a) Experimental amplitude information for x and y axes of Right AMB

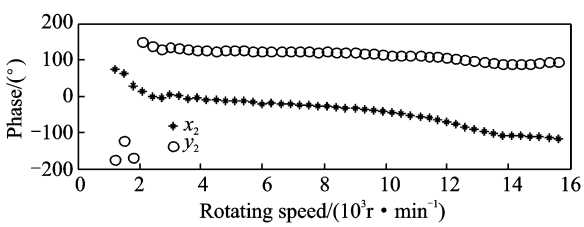

(b) Experimental phase information for x and y axes of Right AMB

Fig. 6 Experimental amplitude and phase information for x and y axes of Right AMB

The threaded holes are designed to add unbalance mass near the supporting position, as

shown in Fig. 7.

According to the unbalance response amplitude and phase obtained from the experiment, the AMB supporting parameters are obtained using hybrid GA. The identification process is shown in Fig. 4 and the identified supporting parameters for the two AMBs are shown in Figs. 8, 9. Here, K_{xx_1}, K_{yy_1}, K_{xx_2} and K_{yy_2} are the stiffness values at each AMB for two orthogonal direction and C_{xx_1}, C_{yy_1}, C_{xx_2} and C_{yy_2} the damping values at each AMBs for two orthogonal direction.

As shown in Figs. 8, 9, the stiffness and damping identified from the right AMB is bigger than that of the left one due to the different control gain of the PID controller in each channel. The AMB stiffness coefficients increase with the speed increasing and the damping parameters remain relatively steady with the speed increasing.

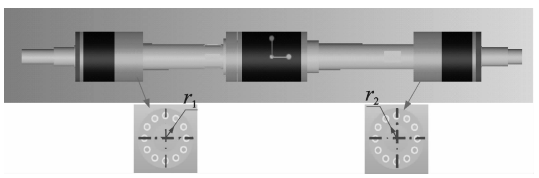

Fig. 7 Test rig rotor for measurements of imbalance responses

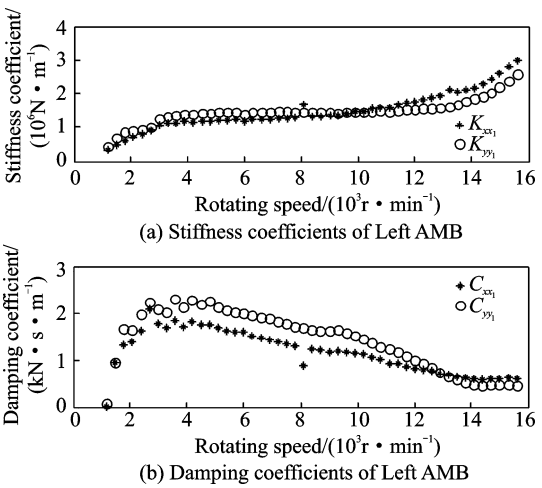

Fig. 8 Stiffness and damping coefficients of Left AMB

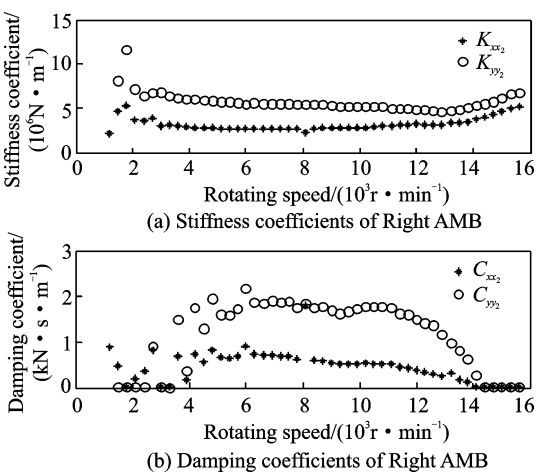

Fig. 9 Stiffness and damping coefficients of Right AMB

3 Verification by Simulation

To verify the identified results, we compare with the results from experiment and simulation. The process of verification by simulation is shown in Fig. 10.

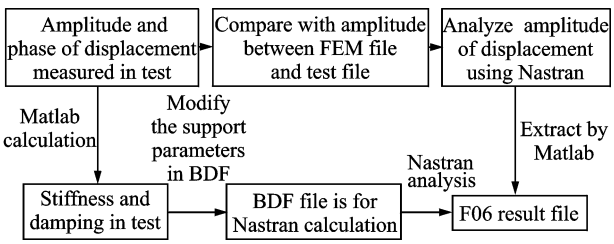

Fig. 10 Process of verification by simulation

The rotor bearing model is built in the finite element software MSC. Patran and the specific dimensions are shown as Fig. 4. The rotor is divided into 436 elements. For silicon steel and copper sleeves, etc. on the shaft, use Lumped Mass modules and plus lumped mass and rotational inertia on shaft. Use bush element to simulate the supporting bearing part. Modify the supporting parameters in BDF file and load unbalance excitation at the position corresponding to the unbalanced mass location of the test. And the finite element model of the rotor is shown in Fig. 11

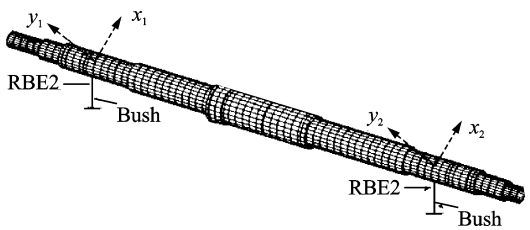

Fig. 11 Finite element model of rotor

During the verification, the identified parameters are employed in the rotor finite element

model as stiffness and damping to calculate the rotor unbalance responses. Because these identified stiffness and damping values vary along with the rotating speed, the Matlab program is adopted as master software to control Nastran to calculate the corresponding unbalance response from 1 200 r/min to 15 600 r/min by 600 r/min. Finally, the comparison between experimental and simulated responses is shown in Figs. 12,13.

From Figs. 12,13, They can be seen that the unbalance response calculated in finite element model basically consistent with the experimental data. This demonstrates that the identification method proposed in this paper is effective.

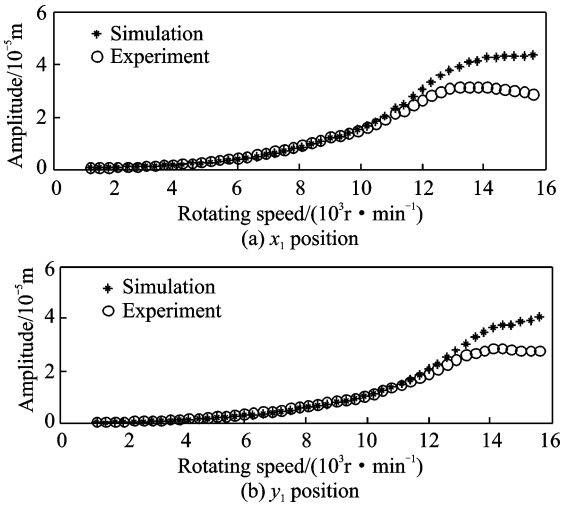

Fig. 12 Comparison between simulation and experiment of Left AMB

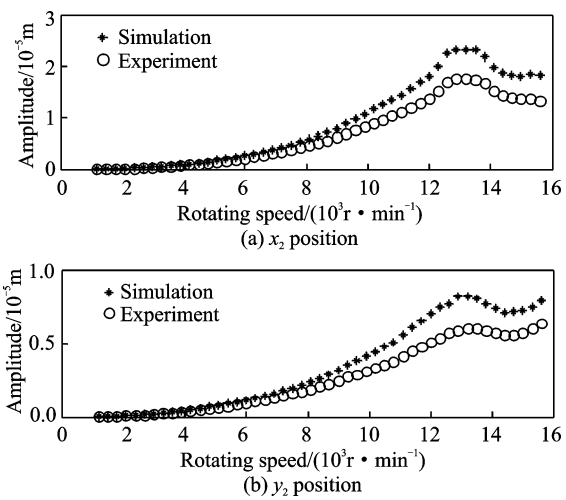

Fig. 13 Comparison between simulation and the experiment of Right AMB

4 Conclusions

An hybrid GA is proposed and employed to identify the AMB stiffness and damping coefficients. This identification algorithm combines both merits of the genetic and simplex optimization algorithm. The proposed method not only can prevent premature of classical GA from falling into local optimum, but also can improve the identification efficiency. The comparison between experimental measurements and finite element simulated response shows that the proposed identification algorithm in the paper can effectively identify the supporting parameters of AMBs.

Acknowledgements

This work was supported by the National Natural Science Foundation of China (No. 51675261) and Jiangsu Province Key R & D Programs (No. BE2016180).

References:

[1] LEE C W, HONG S W. Identification of bearing dynamic coefficients by unbalance response measurement [J]. Journal of Mechanical Engineering Science, 1989, 203(2): 93-101.

[2] SANTIAGO D, ANDRÉS L S. Field method for identification of bearing support parameters—Part II: Identification from rotor dynamic response due to imbalances[J]. Journal of Engineering for Gas Turbines and Power, 2007, 129(1): 213-219.

[3] ANDRÉS L S, SANTIAGO D. Identification of bearing force coefficients from measurements of imbalance response of a flexible rotor[C]// ASME. Vienna: ASME, 2004: 14-17.

[4] TIWARI R, CHAKRAVARTHY V. Identification of the bearing and unbalance parameters from run-down data of rotors[C]// IUTAM Symposium on Emerging Trends in Rotor Dynamics. New Delhi: [s. n.], 2011, 1011: 479-489.

[5] KNAAPEN R J W. Experimental determination of rolling element bearing stiffness [D]. Eindhoven: Eindhoven University of Technology Faculty of Mechanical Engineering Department of Engineering Dynamics, 1997.

[6] JIANG Kejian, ZHU Changsheng. On-line measurement of supporting characteristics of an active magnetic levitations with unknown transfer function[J]. China Mechanical Engineering, 2010, 21(8): 883-888. (in Chinese)

[7] ZHAO Lei, CONG Hua, ZHAO Hongbin. Study on stiffness and damping characteristic of active magnetic bearing[J]. Tsinghua Univ(Sci & Tech), 1999, 39(4): 96-99. (in Chinese)

[8] HU Yefa, WANG Xiaoguang, WU Huanchun. Research and simulation of supportive characteristics of active magnetic bearing[J]. Journal of WUT(Information & Management Engineering), 2001, 23(4): 96-99. (in Chinese)

[9] ZHOU Jin, NI Zuoxi. Identification method for stiffness and damping of magnetic bearings based on rotor unbalance responses[J]. Journal of Vibration and Shock, 2013, 32(3): 29-34. (in Chinese)

[10] YING Guangyao, ZHENG Shuiying, LIU Sulian. Application of genetic algorithm in the rotor-bearing system parameter identification[J]. Journal of Mechanical Strength, 2004, 26(1): 6-9. (in Chinese)

[11] JI Minlai. Test method and identification method of stiffness and damping of magnetic bearings[D]. Nanjing: Nanjing University of Aeronautics and Astronautics, 2013. (in Chinese)

[12] JIN Mingfan, ZHAO Mei. Identification of support stiffness's in rotor-bearing system using genetic algorithm[J]. Journal of Mechanical Strength, 2002, 24(3): 327-330. (in Chinese)

[13] KIM Y H, YANG B, TAN A. Bearing parameter identification of rotor-bearing system using clustering-based hybrid evolutionary algorithm[J]. Struck Multidisc Optim, 2007, 33(6): 493-506.

[14] HAN Wei, LIAO Zhenpeng. A global optimization algorithm: Genetic algorithm-simple [J]. Journal of Earthquake Engineering and Engineering Vibration, 2001, 21(2): 470-475. (in Chinese)

[15] WEN Bangchun, GU Jianiu, XIA Songbo. Advanced rotor dynamic—Thoery, technology and application [M]. Beijing: China Machine Press, 1999. (in Chinese)

[16] JIN C Y, ZHU Y, XU Y, et al. Dynamics of rotor drop on new type catcher bearing[J]. Transactions of Nanjing University of Aeronautics and Astronautics, 2014, 31(1): 70-77.

[17] JIN C, XU L. Measurement error of displacement sensors for active magnetic bearing[J]. Journal of Nanjing University of Aeronautics & Astronautics. 2009, 41(5): 626-632.

[18] XU Yuanping, ZHOU Jin, DI Long, et al. Active magnetic bearing rotor model updating using resonance and MAC error[J]. Shock and Vibration, 2015, 2015: 1-9.

Mr. **Zhao Chen** was born in 1989. He received B. S. degree in College of Mechanical Engineering from Yang Zhou University. And he received M. S. degree in College of Mechanical and Electrical Engineering from Nanjing University of Aeronautics and Astronautics (NUAA).

Prof. **Zhou Jin** received Ph. D. degree in Mechanical Engineering from China University of Mining and Technology (CUMT) in 2001. From 2011 to 2012, she was a visiting scholar in the Rotating Machinery and Control Laboratory (ROMAC) of University of Virginia. She is currently a full professor in College of Mechanical and Electrical Engineering, Nanjing University of Aeronautics and Astronautics (NUAA). Her research focuses on magnetic bearings and vibration control.

Mr. **Xu Yuanping** was born in 1989. He received B. S. degree in College of Mechanical and Electrical Engineering from Nanjing University of Aeronautics and Astronautics (NUAA) in 2012. He is currently a Ph. D. candidate in NUAA and a guest Ph. D. candidate in Ecole Polytechnique Federale Lausanne (EPFL), Switzerland. His research focuses on magnetic levitation.

Dr. **Di Long** received his B. S. and M. S. degrees, both in Electrical Engineering from Utah State University, Logan, UT, in 2009 and 2011, respectively. He obtained his Ph. D. degree at University of Virginia in 2016. His main research interest lies in modeling and control of active magnetic bearings.

Mr. **Ji Minlai** received his M. S. degree in College of Mechanical and Electrical Engineering from Nanjing University of Aeronautics and Astronautics (NUAA). Now he works in AVIC radar and electronic equipment research institute.

(Executive Editor: Xu Chengting)